

Unravelling structural insight into optical properties of a pair of aza-BODIPY isomers and application for photodynamic therapy

Di Tao,^{‡,a} Chenshuang Dong,^{‡,b} Yanru Huang,^a Yunsheng Xue,^c Yuehong Zhang,^a
Guiling Wang,^{*b} Xin-Dong Jiang,^{*a} Gaowu Qin^{*a}

1. Experiment
2. NMR
3. HRMS
- 4 Table
5. Figure
6. X-ray data
7. Cartesian coordinates
8. Reference

1. Experiment

1.1 General

Unless otherwise noted, all chemical reagents and organic solvents were of analytical quality and obtained from Energy Chemical & Technology (Shanghai) Co. Ltd. without extra purification. A VARIAN Mercury 500 MHz spectrometer has been employed to record ^1H NMR spectra. Determined ^1H NMR chemical shifts (δ) from Me_4Si are presented in ppm downfield by trace amounts of chloroform (7.26 ppm). On a VARIAN Mercury 125 MHz spectrometer, ^{13}C NMR spectra were obtained in CDCl_3 , reporting in ppm with the internal chloroform signal at $\delta = 77.0$ ppm as the reference. The precise molecular weight of the product was determined using a high resolution mass spectrometer. At 298 K, an absorption spectrogram was taken using a UV-2550 spectrophotometer. Utilizing an F-128 spectrophotometer, fluorescence spectra have been recorded and displayed as cm^{-1} . The F-98 spectrophotometer was used for measuring the absolute fluorescence quantum yield. A temperature-measuring camera maintains record of the solution temperatures. A fiber connected laser system was implemented to control a 915 nm laser, which was deployed as the light source for the light irradiation and was bought from Changchun New Industries Optoelectronics Technology. A CEL-NP 2000 power meter was used to test the optical power density, it was bought from Beijing Zhong Jiao Jin Yuan Technology Co, Ltd. The CCK8 assay was via BioTek Synergy H1 microplate reader. To estimate fluorescence visualization, a Confocal Laser Fluorescence Microscope FV1200 (Olympus, Japan) was employed.

1.2 Computational method

All calculations have been performed by using the Gaussian 09 programs ^[1]. Geometrical structures were optimized using the DFT method with the hybrid functional PBE0 ^[2] and TZVP basis set. Vibrational frequencies were calculated at the same level to characterize the stationary point as minima points. The vertical transition energies were calculated using the TDDFT method with PBE0 and TZVP basis set. Solvent effects were simulated using the polarizable continuum model

(PCM) [3, 4]. NCI (noncovalent interactions) analysis was performed by Multiwfn program [5] according to the previously described methodology [6]. VMD software [7] was used to generate the NCI plots.

1.3 Singlet oxygen detection

Utilizing 1,3-diphenylisobenzofuran (DPBF), the $^1\text{O}_2$ production in toluene was determined. The absorbance of DPBF at 416 nm was adjusted to about 1.5 in toluene and the absorbance of dye molecule was adjusted to about 0.8. The characteristic absorption of DPBF was applied to characterize $^1\text{O}_2$ production. The absorption value of the dye molecule indicates the photo-stability of the dye. The 808 nm laser light source is used, the optical radiation power is 0.1 W/cm^2 , and the illuminated time is 0-17 min.

The $^1\text{O}_2$ production efficiency of the dyes can be calculated by the following formula under the reference of methylene blue (MB) with known $^1\text{O}_2$ production rate efficiency (57% in DCM solution).

$$\Phi_{\text{sam}} = \Phi_{\text{MB}} \left(\frac{m_{\text{sam}}}{m_{\text{MB}}} \right) \left(\frac{F_{\text{MB}}}{F_{\text{sam}}} \right)$$

Where “sam” represents the unknown dye molecule and “MB” represents the reference methylene blue. “m” is the slope of DPBF absorption peak decline, “F” is the absorption correction factor, $F = 1 - 10^{-\text{O.D.}}$. O.D. represents the absorption value of the sample at the wavelength of light radiation.

1.4 Calculation of photothermal efficiency

The photothermal conversion efficiencies (η) was calculated using the following method:

$$\eta = \frac{hs(T_{\text{Max}} - T_{\text{Surr}}) - Q_{\text{Dis}}}{I(1 - 10^{-A})}$$

h means heat transfer coefficient, s was for container surface area, Q_{Dis} stands for heat dispersed from the laser via the solvent and container, I was for laser power, and A represents for absorbance at excitation wavelength. η denotes photothermal conversion efficiency.

$$hs = \frac{mC}{\tau_s}$$

m is the total quantity of the photothermal reagent containing solution, C represents the temperature coefficient, and τ_s is the relevant time constant.

$$t = -\tau_s \ln(\theta)$$

The temperature of the driving force is a non-dimensional parameter termed θ .

$$\theta = \frac{T - T_{Surr}}{T_{Max} - T_{Surr}}$$

T is the current temperature, T_{Max} is the highest steady state temperature, and T_{Surr} denotes the surrounding temperature.

1.5 CCK8 Cytotoxicity Assay

Human colorectal cancer (HCT116) cells were seeded in a 96-well plate. To determine the optimal concentration of dye NPs, various concentration gradients (0-40 μM) were added to the light exposure group and the dye NPs plus light exposure group. After treatment with the photosensitizer, the cells were incubated for 2 hours and then irradiated with 635 nm radiation (0.8 W cm^{-2} , 20 min). Subsequently, the Cell Counting Kit-8 (CCK8) was added to each well, followed by a further 2-hour incubation. The absorbance at 450 nm was measured using a microplate reader. Cell viability (%) = $(\text{OD}_{\text{dye}} - \text{OD}_{\text{blank}}) / (\text{OD}_{\text{control}} - \text{OD}_{\text{blank}}) \times 100\%$.

1.6 AM/PI Dual-Staining of Live-Dead Cells

Human colorectal cancer (HCT116) cells were seeded in a 24-well plate. To observe the dark and phototoxicity of dye NPs, cells were divided into several groups for treatment. Control group, 30 μM dye NPs treatment group, 635 nm light exposure group; 635 nm light exposure + 30 μM dye NPs group. The experiment used a Calcein-AM/PI dual-staining kit, and after a 30-minute incubation, confocal fluorescence imaging was performed. Calcein AM exhibits green fluorescence to indicate live cells, while PI emits red fluorescence, indicating dead cells.

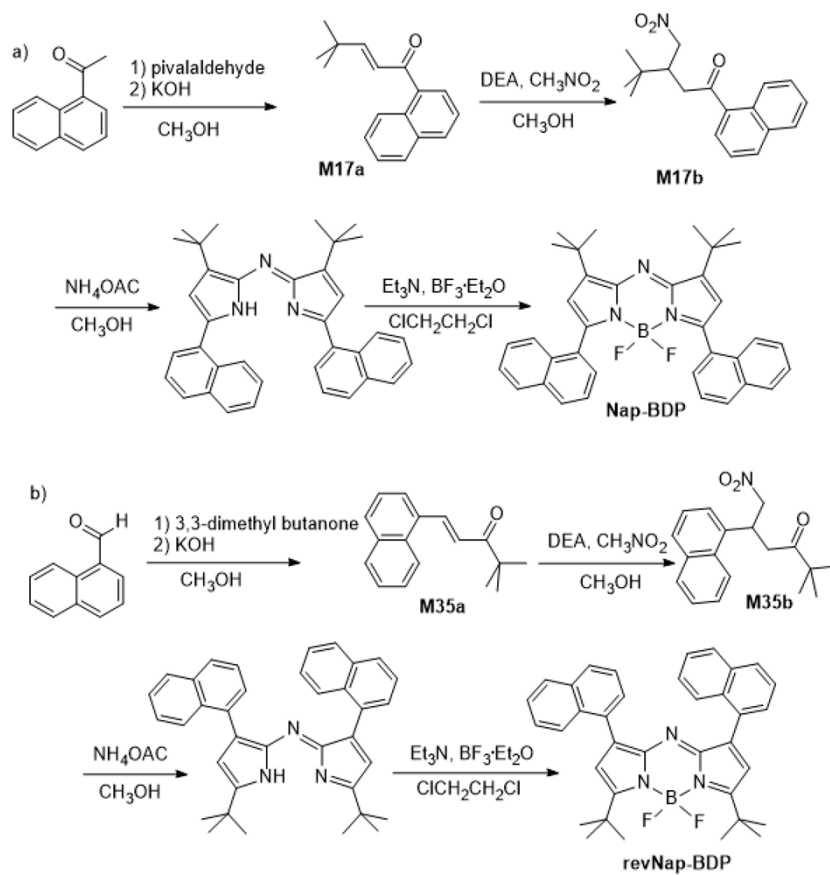
1.7 Apoptosis Detection

Apoptosis detection was performed using four groups of cells: control group, light exposure group, dye NPs group, and dye NPs + light exposure group. After a 2-hour treatment, cells were collected using trypsin without EDTA, and $1 \times 10^5 \sim 5 \times 10^5$ cells were counted and added to Bind Buffer to form a single-cell suspension. Then, 5 μ l Annexin V-FITC and 10 μ l PI were added, and the mixture was incubated at room temperature in the dark for 10 minutes, followed by flow cytometry analysis within 1 hour.

1.8 ROS Detection

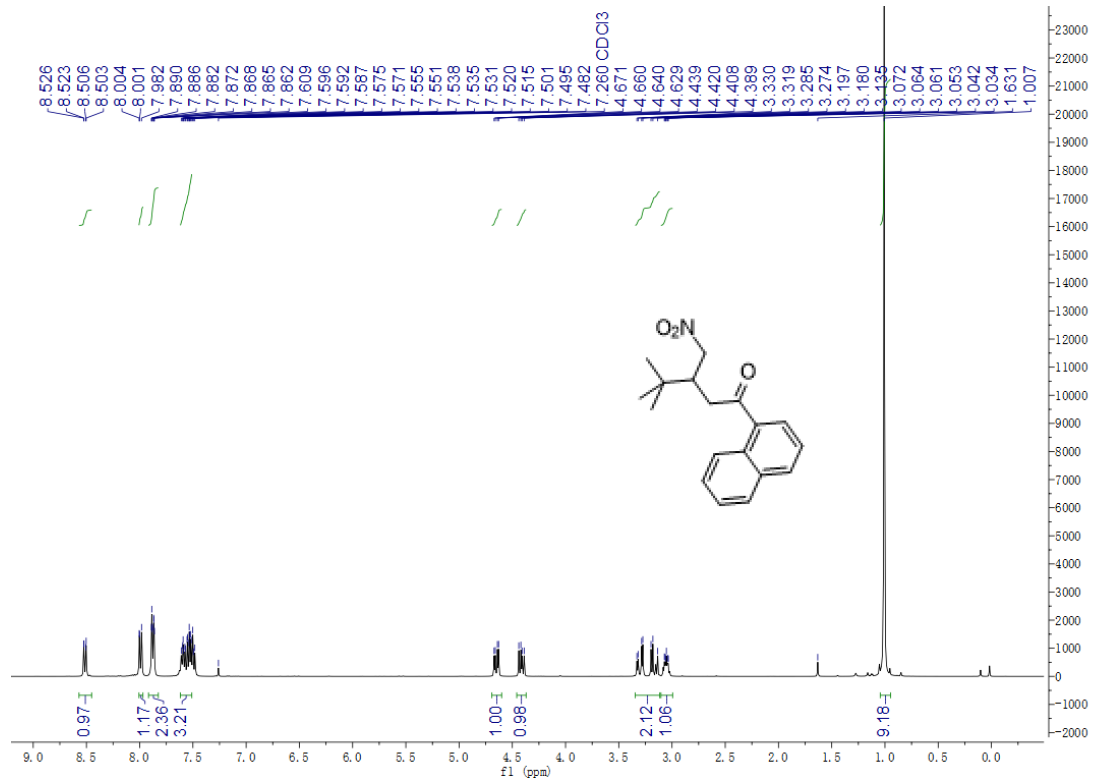
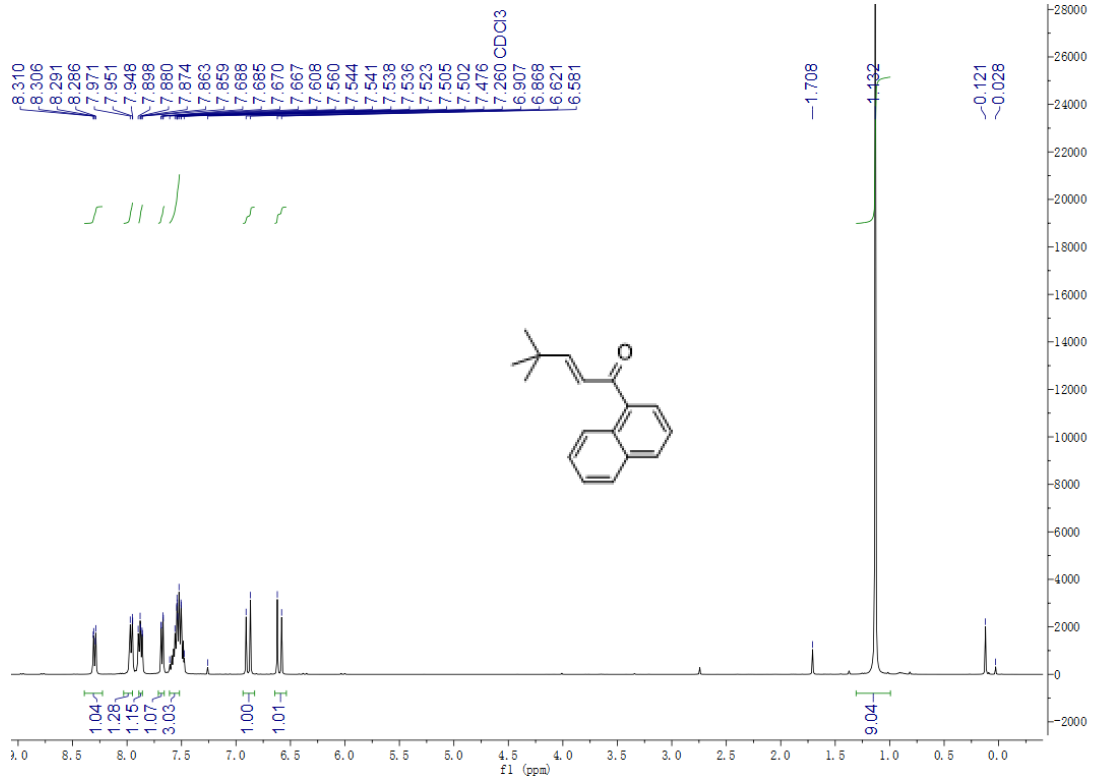
ROS detection was performed using four groups of cells: control group, light exposure group, dye NPs group, and dye NPs + light exposure group. Cells were seeded at a density of $10^5 \sim 10^6$ in a six-well plate. After a 2-hour treatment, the DCFH-DA probe was added, and the cells were incubated at 37 °C for 30 minutes. Cells were then collected using trypsin, forming a single-cell suspension, and centrifuged for 5 minutes. The cells were washed three times with PBS. Flow cytometry analysis was performed within 1 hour.

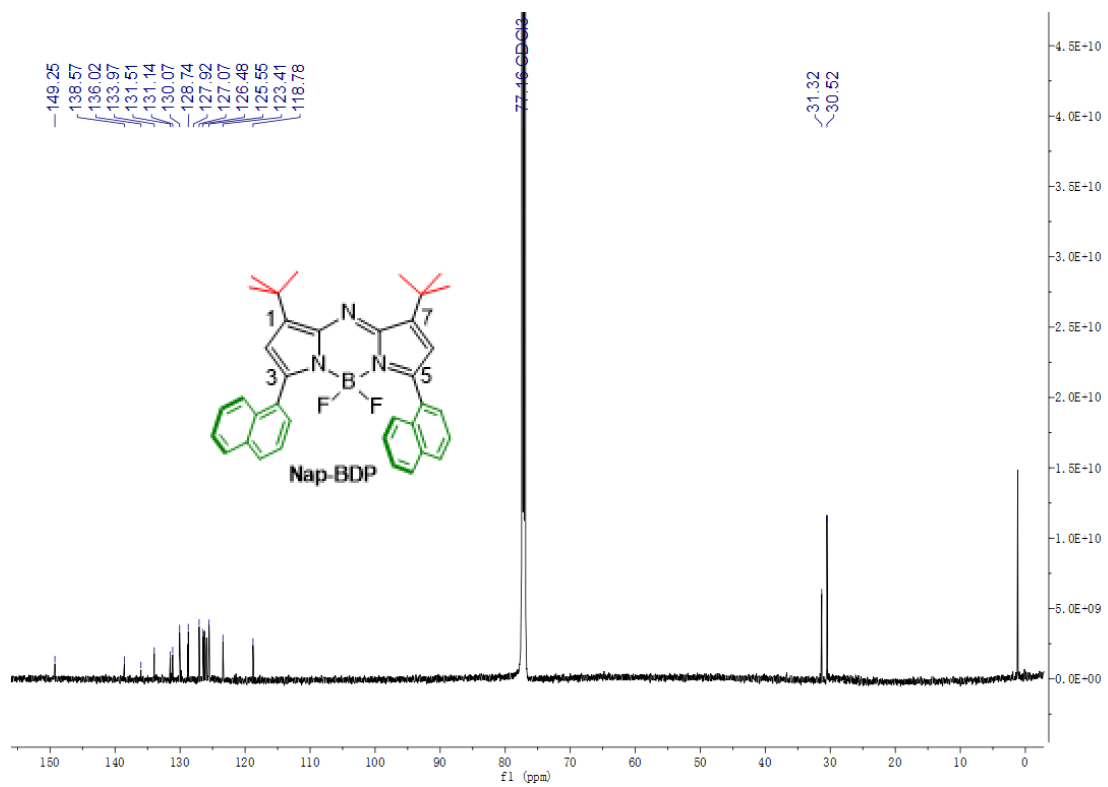
1.9 Synthetic route



Scheme S1

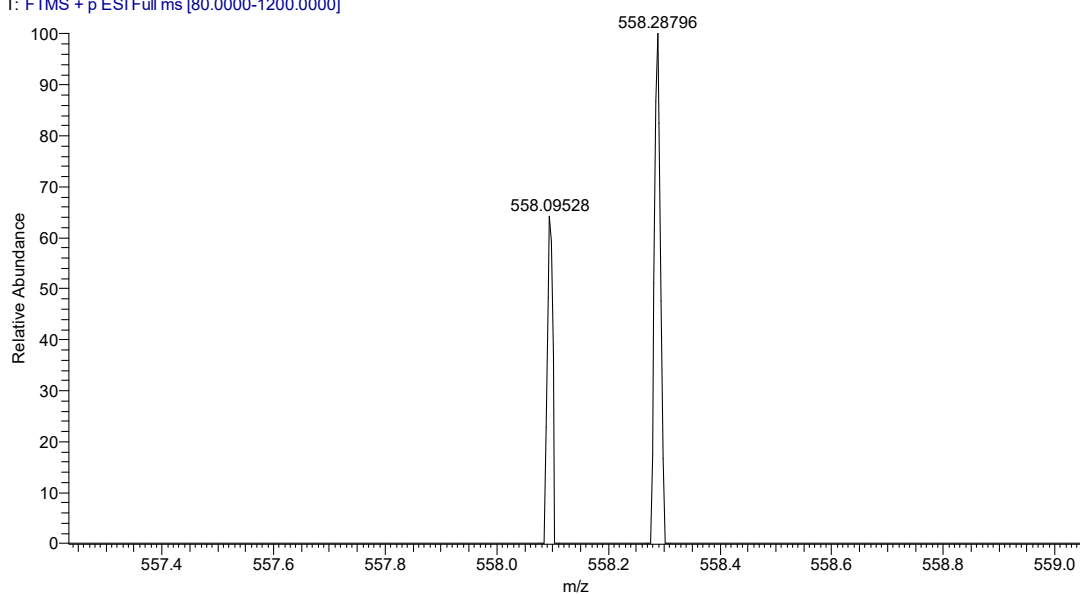
2. NMR





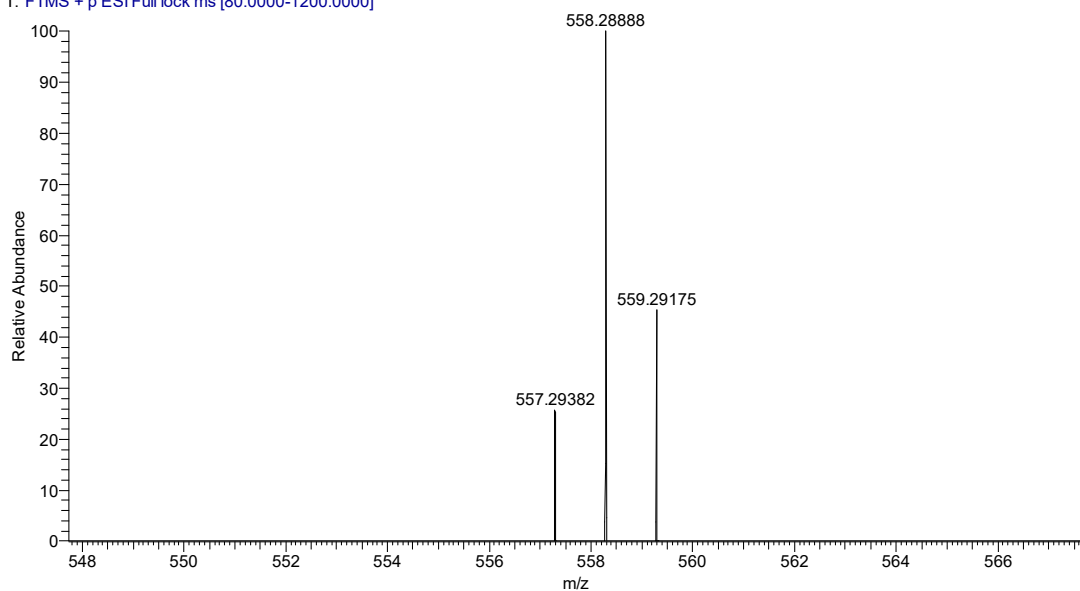
3. HRMS

64-5 #32 RT: 0.27 AV: 1 NL: 1.10E3
T: FTMS + p ESI Full ms [80.0000-1200.0000]



Nap-BDP: HRMS (ESI) m/z calcd for $C_{36}H_{35}BF_2N_3^+$ (M+H)⁺ 558.28866, found 558.28796.

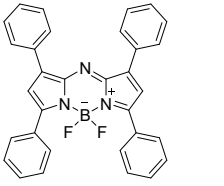
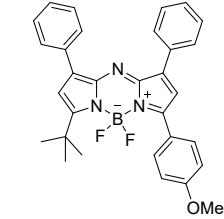
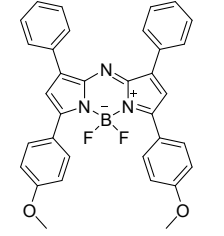
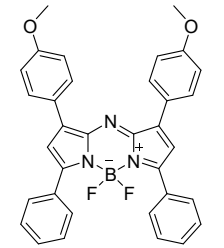
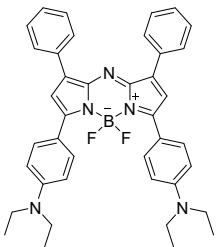
188-TD-315-582 #15 RT: 0.09 AV: 1 NL: 9.76E5
T: FTMS + p ESI Full lock ms [80.0000-1200.0000]

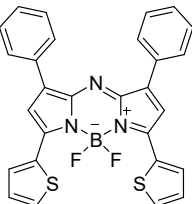
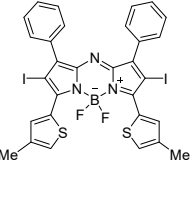
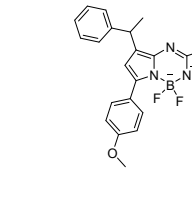
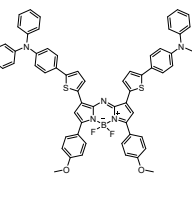
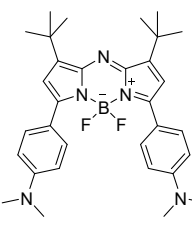
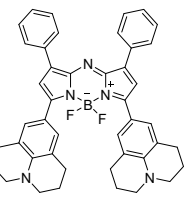


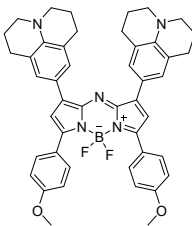
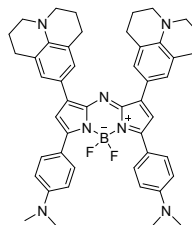
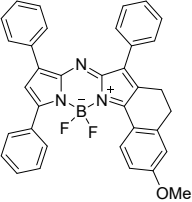
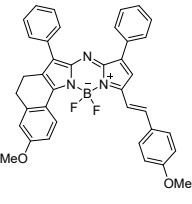
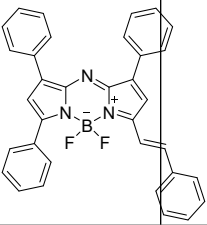
revNap-BDP: HRMS (ESI) m/z calcd for $C_{36}H_{35}BF_2N_3^+$ (M+H)⁺ 558.28866, found 558.28888.

4. Table

Table S1 Structures and application of the reported aza-BODIPYs.

Dyes	$\lambda_{\text{abs}}/\lambda_{\text{em}}$ (nm)	Applicaion	Reference
	640/661	$\Phi_{\text{F}}=0.34$ $\eta=38\%$ $\Phi_{\Delta}=0.02$	<i>J. Mater. Chem.B</i> , 2024, 12 ,1372-1378.
	636/665	$\Phi_{\text{F}}=0.15$ $\eta=43\%$ $\Phi_{\Delta}=0.027$	<i>J. Mater. Chem.B</i> , 2022, 10 ,8443-8449.
	688/724	$\Phi_{\text{F}}=0.36$ $\eta=39\%$ $\Phi_{\Delta}=0.021$	<i>J.Mater. Chem. B</i> , 2024, 12 ,1372-1378.
	664/691	$\Phi_{\text{F}}=0.23$ $\Phi_{\Delta}=0.08$	<i>Eur. J. Org. Chem.</i> 2020, 971–977.
	818/850	$\Phi_{\text{F}}=0.013$ $\Phi_{\Delta}=0.026$	<i>ACS Chem. Biol.</i> 2018, 13 , 1838–1843.

	717/741	$\Phi_F=0.24$ $\eta=66\%$ $\Phi_\Delta=0.004$	<i>Chem. Sci.</i> , 2024, 15 , 5973.
	732/768	$\Phi_F=0.07$ $\Phi_\Delta=0.14$	<i>J. Med. Chem.</i> 2020, 63 , 9950–9964.
	674/715	$\Phi_F=0.19$ $\eta=48.6\%$ $\Phi_\Delta=0$	<i>Chin. Chem. Lett.</i> , 2024, 35 , 110460.
	850/1000	$\eta=35\%$	<i>Talanta</i> 2024, 279 , 126633.
	748/805	$\eta=49.3\%$ $\Phi_\Delta=0$	<i>J. Mater. Chem. B</i> , 2023, 11 , 10625.
	906/1023	$\Phi_F=0.001$ $\eta=79\%$ $\Phi_\Delta=0.02$	<i>ACS Materials Lett.</i> 2024, 6 , 4765–4773.

	910/1060	$\Phi_f=0.001$ $\Phi_{\Delta}=0$ $\eta=61\%$	<i>Chem. Commun.</i> , 2019, 55 , 10920-10923.
	862/998	$\Phi_f=0.003$ $\eta=50.5\%$ $\Phi_{\Delta}=0$	<i>Chin. Chem. Lett.</i> , 2024, 35 , 109735.
	690/716	$\Phi_f=0.44$ $\eta=43.5\%$ $\Phi_{\Delta}=0.011$	<i>J.Mater.Chem.B</i> , 2022, 10 ,8443-8449.
	746/765	$\Phi_f=0.12$ $\Phi_{\Delta}=0.034$	<i>Dyes Pigm</i> , 2022, 198 , 110026.
	686/709	$\Phi_f=0.22$ $\Phi_{\Delta}=0.043$	<i>Dyes Pigm</i> , 2022, 198 , 110026.

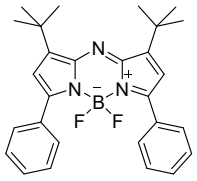
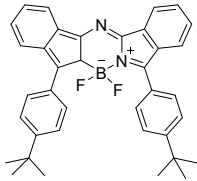

	620/650	$\Phi_F=0.11$ $\eta=47\%$ $\Phi_\Delta=0.035$	<i>Chem. Eur. J.</i> 2022, 28 , e202103571.
	662/677	$\Phi_F=0.13$ $\Phi_\Delta=0.041$ $\eta=48.1\%$	<i>J. Mater. Chem. B</i> , 2022, 10 ,8443-8449.
 <p>Nap-BDP</p>	604/667	$\Phi_F=0.13$ $\Phi_\Delta=0.349$	<i>This work</i>

Table S2 Photophysical properties of **Nap-BDP** and **revNap-BDP** in various solvents at 298 K.

solvent	Nap-BDP				revNap-BDP			
	$\lambda_{\text{abs}}/\lambda_{\text{em}}$	FWHM	Stokes shift	ϕ	$\lambda_{\text{abs}}/\lambda_{\text{em}}$	FWHM	Stokes shift	ϕ
DMF	604/672	72	68	0.09	584/681	46	97	0.22
DMSO	606/675	74	69	0.08	584/683	50	99	0.21
DCM	604/667	68	63	0.13	584/663	44	79	0.29
toluene	612/671	72	59	0.12	584/657	48	73	0.27
PE	608/661	68	53	0.12	580/640	42	60	0.27
THF	606/669	68	63	0.13	584/663	46	79	0.28
ACN	596/663	70	67	0.13	580/676	40	96	0.27
EAC	604/665	64	61	0.12				
CHCl ₃					584/655	46	71	0.27

Table S3. Calculated maximum absorption wavelength $\lambda_{\text{max,ab}}$ (eV, nm), oscillator strength (f) and transition assignment.

Molecule	state	E (eV)	$\lambda_{\text{max,ab}}$ (nm)	f	Assignment	Exp. (nm)
revNap-BDP	S ₁	2.1671	572.11	0.4194	HOMO→LUMO	584
Nap-BDP	S ₁	2.1182	585.33	0.7403	HOMO→LUMO	603

Table S4. Excitation energies (eV) of the low-lying excited states and spin-orbit coupling constants ($\zeta(S_n, T_n)$) between them based on the optimized S₀-geometries of **revNap-BDP** and **Nap-BDP**.

Dye	S ₁	S ₂	T ₁	T ₂	T ₃	$\Delta E(S_1-T_3)$	$\Delta E(S_1-T_1)$	ζ_{soc} (cm ⁻¹)
revNap-BDP	2.1671	3.6951	0.9261	1.9775	2.0226	0.1445		0.4818
Nap-BDP	2.1182	2.6810	0.8322	2.2451	2.3749		1.2953	0.0141

5. Figure

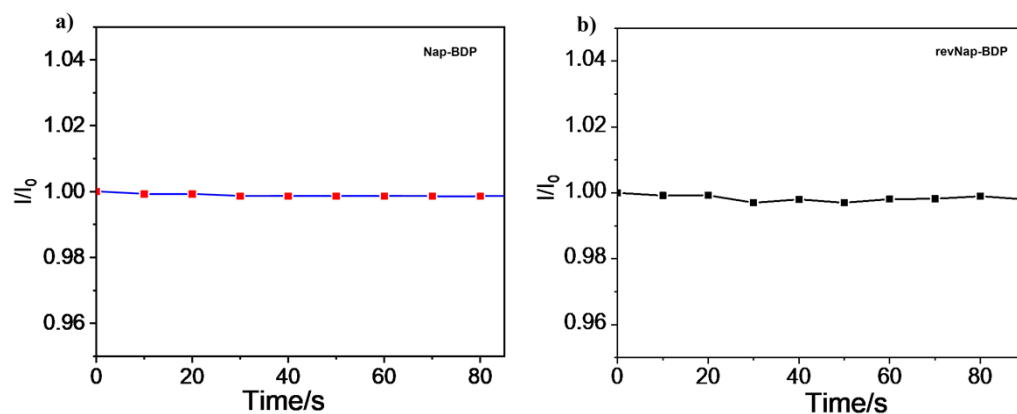


Fig. S1 ROS generation of **Nap-BDP** (5 μ M) or **revNap-BDP** (5 μ M) in THF under continuous 635 nm laser (0.1 W/cm²) irradiation for 1.5 min using dihydrorhodamine 123 (DHR123) (10 μ M) as an indicator.

Fig. S2 a) Absorption of **Nap-BDP** NPs in aqueous solution at 298 K. b) Absorption spectra of **Nap-BDP** in different proportions of water (0–100%) in THF solution.

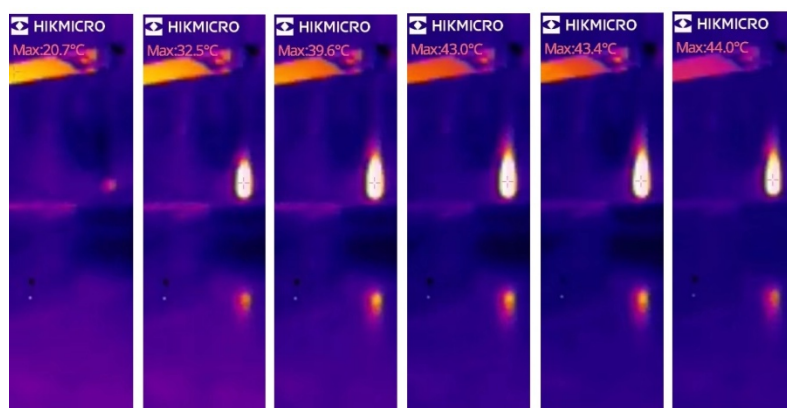


Fig. S3 Photothermal images (20.7–44.0 °C) of **Nap-BDP** NPs in water

under 635 nm laser irradiation (0.8 W cm^{-2} , 5 min).

Fig. S 4 a) DLS of **revNap-BDP** NPs in aqueous solution. b) Temperature changes of **revNap-BDP** NPs at different concentrations (20–80 μM) under 635 nm laser irradiation (0.8 W cm^{-2}). c) Photothermal conversion of **revNap-BDP** NPs (80 μM) under 635 nm laser irradiation with different power density ($0.2\text{--}0.8 \text{ W}\cdot\text{cm}^{-2}$). d) Photothermal stability study during five circles of heating-cooling processes. e) Temperature response curves of **revNap-BDP** NPs in aqueous solutions under irradiation and naturally cooling. i) Linear fitting of $-\ln(\theta)$ and time.

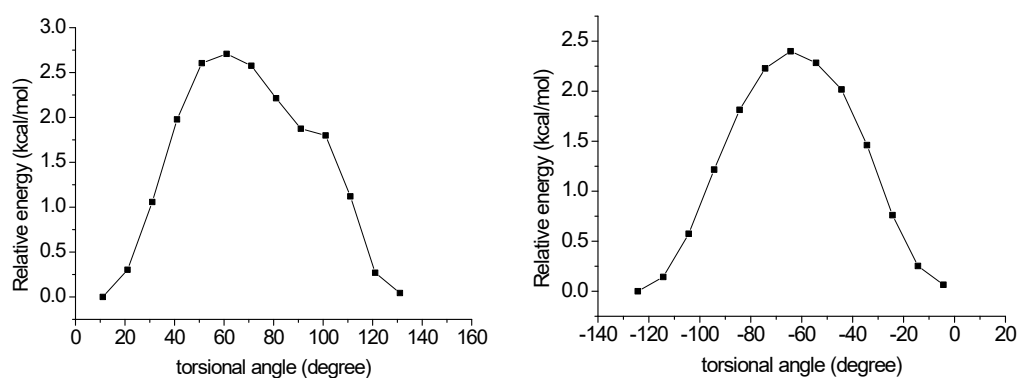


Fig. S5 Potential curve of the torsion angles of tertiary butyl group in **revNap-BDP** (left) and **Nap-BDP** (right). The rotational barriers are 2.71 and 2.40 kcal/mol, respectively.

6. Xray data

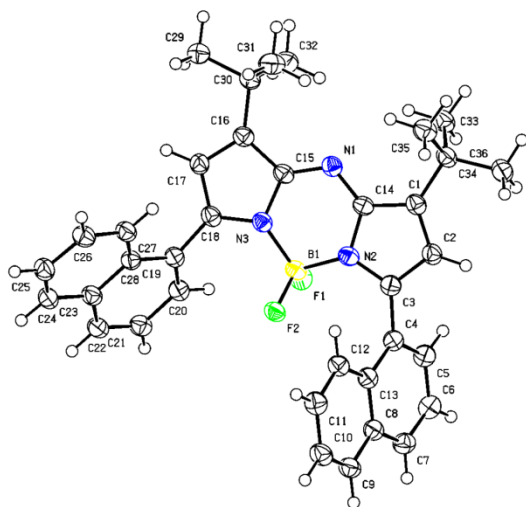


Table 1 Crystal data and structure refinement for td-17-2.

Identification code	td-17-2
Empirical formula	C ₃₆ H ₃₄ BF ₂ N ₃
Formula weight	557.47
Temperature/K	118(20)
Crystal system	triclinic
Space group	P-1
a/Å	7.6796(3)
b/Å	9.3847(3)
c/Å	20.7610(7)
α /°	77.492(3)
β /°	89.674(3)
γ /°	89.190(3)
Volume/Å ³	1460.60(9)
Z	2
$\rho_{\text{calc}}/\text{cm}^3$	1.268
μ/mm^{-1}	0.659
F(000)	588.0
Crystal size/mm ³	0.14 × 0.12 × 0.11
Radiation	Cu K α (λ = 1.54184)
2 θ range for data collection/°	8.726 to 148.574
Index ranges	-8 ≤ h ≤ 9, -11 ≤ k ≤ 11, -25 ≤ l ≤ 25
Reflections collected	14754
Independent reflections	5652 [R _{int} = 0.0401, R _{sigma} = 0.0537]
Data/restraints/parameters	5652/0/385
Goodness-of-fit on F ²	1.037
Final R indexes [I >= 2 σ (I)]	R ₁ = 0.0578, wR ₂ = 0.1575

Final R indexes [all data] $R_1 = 0.0692$, $wR_2 = 0.1687$

Largest diff. peak/hole / $e \text{ \AA}^{-3}$ 0.35/-0.27

Crystal structure determination of [td-17-2]

Crystal Data for $C_{36}H_{34}BF_2N_3$ ($M=557.47$ g/mol): triclinic, space group P-1 (no. 2), $a = 7.6796(3)$ \AA , $b = 9.3847(3)$ \AA , $c = 20.7610(7)$ \AA , $\alpha = 77.492(3)^\circ$, $\beta = 89.674(3)^\circ$, $\gamma = 89.190(3)^\circ$, $V = 1460.60(9)$ \AA^3 , $Z = 2$, $T = 118(20)$ K, $\mu(\text{Cu K}\alpha) = 0.659$ mm^{-1} , $D_{\text{calc}} = 1.268$ g/cm^3 , 14754 reflections measured ($8.726^\circ \leq 2\Theta \leq 148.574^\circ$), 5652 unique ($R_{\text{int}} = 0.0401$, $R_{\text{sigma}} = 0.0537$) which were used in all calculations. The final R_1 was 0.0578 ($I > 2\sigma(I)$) and wR_2 was 0.1687 (all data).

Table 2 Fractional Atomic Coordinates ($\times 10^4$) and Equivalent Isotropic Displacement Parameters ($\text{\AA}^2 \times 10^3$) for td-17-2. U_{eq} is defined as 1/3 of the trace of the orthogonalised U_{ij} tensor.

Atom	x	y	z	U(eq)
F1	-1120.9(15)	2786.2(12)	7645.6(5)	35.0(3)
F2	256.9(15)	3874.7(12)	6696.1(5)	32.9(3)
N1	2006(2)	4848.7(17)	8419.5(7)	28.6(4)
N2	-146(2)	5246.8(17)	7556.8(7)	28.7(4)
N3	1970(2)	3194.9(16)	7686.9(7)	27.9(3)
C1	-81(3)	6923(2)	8217.5(9)	29.0(4)
C2	-1405(3)	7283(2)	7764.3(9)	30.5(4)
C3	-1446(3)	6245(2)	7366.8(9)	28.9(4)
C4	-2781(3)	6170(2)	6865.3(9)	29.4(4)
C5	-4481(3)	6002(2)	7078.0(9)	33.5(4)
C6	-5851(3)	5913(2)	6644.3(10)	35.2(4)
C7	-5507(3)	6018(2)	5989.4(10)	34.3(4)
C8	-3791(3)	6259(2)	5738.0(9)	30.0(4)
C9	-3443(3)	6468(2)	5051.5(9)	34.7(4)
C10	-1790(3)	6732(2)	4812.1(9)	36.9(5)
C11	-421(3)	6820(2)	5245.7(10)	35.8(5)
C12	-701(3)	6638(2)	5910.7(9)	30.8(4)
C13	-2399(3)	6333.9(19)	6178.4(9)	29.4(4)
C14	700(2)	5621(2)	8091.2(8)	28.0(4)
C15	2628(3)	3689(2)	8229.5(8)	28.6(4)
C16	4169(3)	2851(2)	8467.4(9)	29.1(4)
C17	4464(3)	1964(2)	8033.1(9)	30.2(4)
C18	3107(3)	2173(2)	7560.0(9)	29.0(4)

Table 2 Fractional Atomic Coordinates ($\times 10^4$) and Equivalent Isotropic Displacement Parameters ($\text{\AA}^2 \times 10^3$) for td-17-2. U_{eq} is defined as 1/3 of the trace of the orthogonalised U_{ij} tensor.

Atom	x	y	z	U(eq)
C19	2905(3)	1357(2)	7039.4(9)	29.4(4)
C20	1363(3)	666(2)	6975.0(9)	30.9(4)
C21	1211(3)	-273(2)	6535.2(9)	33.3(4)
C22	2611(3)	-517(2)	6162.5(9)	32.8(4)
C23	4211(3)	189(2)	6197.0(9)	31.0(4)
C24	5658(3)	-31(2)	5801.1(9)	33.1(4)
C25	7155(3)	729(2)	5805.4(9)	35.3(4)
C26	7289(3)	1761(2)	6206.9(9)	34.7(4)
C27	5936(3)	1968(2)	6612.4(9)	31.5(4)
C28	4374(3)	1172(2)	6631.5(9)	28.8(4)
C29	6583(3)	1723(2)	9210.4(10)	39.5(5)
C30	5200(3)	2938(2)	9077.4(9)	30.7(4)
C31	6105(3)	4419(2)	8978.6(11)	42.1(5)
C32	3963(3)	2754(3)	9671.2(10)	41.3(5)
C33	305(3)	6637(2)	9425.6(9)	36.3(5)
C34	469(3)	7699(2)	8753.5(9)	31.6(4)
C35	2358(3)	8198(2)	8640.6(10)	37.3(5)
C36	-727(3)	9022(2)	8750.3(10)	40.4(5)
B1	176(3)	3740(2)	7367.2(10)	28.8(4)

Table 3 Anisotropic Displacement Parameters ($\text{\AA}^2 \times 10^3$) for td-17-2. The Anisotropic displacement factor exponent takes the form: $-2\pi^2[h^2a^{*2}U_{11}+2hka^*b^*U_{12}+\dots]$.

Atom	U_{11}	U_{22}	U_{33}	U_{23}	U_{13}	U_{12}
F1	35.0(6)	32.8(6)	37.0(6)	-6.9(5)	3.7(5)	-4.5(5)
F2	42.5(7)	32.5(6)	24.2(5)	-7.6(4)	-2.0(5)	2.2(5)
N1	32.3(9)	29.6(8)	23.1(7)	-3.7(6)	3.6(6)	-1.1(7)
N2	32.1(9)	30.5(8)	23.3(7)	-5.4(6)	0.3(6)	-1.9(7)
N3	32.4(9)	27.1(7)	24.3(7)	-5.5(6)	1.4(6)	-1.2(6)
C1	35.4(11)	27.8(9)	23.0(8)	-3.9(7)	3.8(7)	-1.5(8)
C2	36.5(11)	29.2(9)	25.4(8)	-5.1(7)	2.0(8)	2.5(8)
C3	31.2(10)	30.0(9)	24.3(8)	-2.9(7)	3.3(7)	-1.0(8)
C4	33.3(11)	26.5(9)	27.3(9)	-3.7(7)	0.4(8)	0.1(8)
C5	36.2(11)	34.2(10)	27.7(9)	-1.2(7)	3.6(8)	0.3(8)
C6	33.0(11)	33.9(10)	36.4(10)	-2.6(8)	3.0(8)	-1.6(8)
C7	37.2(11)	29.8(10)	35.2(10)	-5.1(8)	-5.2(8)	-1.1(8)

Table 3 Anisotropic Displacement Parameters ($\text{\AA}^2 \times 10^3$) for td-17-2. The Anisotropic displacement factor exponent takes the form: $-2\pi^2[h^2a^{*2}U_{11}+2hka^*b^*U_{12}+\dots]$.

Atom	U_{11}	U_{22}	U_{33}	U_{23}	U_{13}	U_{12}
C8	34.9(11)	26.3(9)	28.6(9)	-5.2(7)	-0.6(8)	-0.3(8)
C9	44.8(12)	31.4(10)	28.0(9)	-7.0(8)	-5.5(8)	1.2(9)
C10	48.2(13)	36.4(10)	25.1(9)	-4.7(8)	2.2(8)	0.2(9)
C11	41.4(12)	34.4(10)	29.7(9)	-2.6(8)	4.8(8)	-1.6(9)
C12	35.1(11)	29.2(9)	27.5(9)	-4.6(7)	1.4(8)	-2.3(8)
C13	36.1(11)	24.2(8)	26.9(9)	-3.5(7)	0.8(8)	0.2(8)
C14	31.3(10)	30.0(9)	22.1(8)	-4.5(7)	0.8(7)	-2.5(8)
C15	34.3(11)	29.6(9)	21.8(8)	-5.3(7)	1.4(7)	-2.4(8)
C16	33.5(10)	28.3(9)	24.4(8)	-3.5(7)	0.7(7)	-1.8(8)
C17	35.2(11)	29.7(9)	25.5(8)	-5.9(7)	0.9(8)	4.6(8)
C18	36.3(11)	27.1(9)	23.2(8)	-4.5(7)	3.2(7)	-0.9(8)
C19	38.0(11)	25.0(9)	24.4(8)	-3.7(7)	0.0(7)	2.3(8)
C20	35.6(11)	28.3(9)	28.4(9)	-5.2(7)	1.2(8)	-0.4(8)
C21	38.6(11)	30.0(9)	31.1(9)	-6.2(8)	-1.6(8)	-3.0(8)
C22	42.6(12)	28.6(9)	27.8(9)	-7.3(7)	-2.7(8)	0.3(8)
C23	40.2(11)	27.8(9)	24.8(8)	-5.7(7)	-2.0(8)	1.5(8)
C24	42.9(12)	29.4(9)	27.7(9)	-7.8(7)	0.2(8)	3.3(8)
C25	39.4(12)	37.1(10)	29.8(9)	-8.6(8)	3.8(8)	3.2(9)
C26	36.6(11)	38.4(11)	29.7(9)	-8.1(8)	2.1(8)	-3.6(9)
C27	36.7(11)	32.6(10)	25.8(9)	-7.9(7)	-0.3(8)	0.4(8)
C28	34.1(10)	27.9(9)	23.7(8)	-4.6(7)	-1.1(7)	2.7(8)
C29	45.9(13)	41.6(11)	32.0(10)	-10.5(9)	-7.9(9)	7.7(10)
C30	35.3(11)	33.8(10)	23.1(8)	-6.4(7)	0.1(8)	1.0(8)
C31	50.6(14)	38.2(11)	36.7(10)	-6.1(9)	-10.0(10)	-3.6(10)
C32	43.3(13)	53.2(13)	25.3(9)	-4.3(9)	1.3(8)	5.7(10)
C33	48.0(13)	35.8(10)	25.3(9)	-7.0(8)	3.1(8)	0.3(9)
C34	40.9(11)	29.9(9)	24.7(8)	-7.7(7)	1.0(8)	0.7(8)
C35	45.8(13)	32.2(10)	33.9(10)	-6.7(8)	-1.4(9)	-4.2(9)
C36	53.7(14)	35.4(11)	33.6(10)	-11.4(8)	-2.3(9)	7.1(10)
B1	33.2(12)	30.2(10)	23.2(9)	-6.3(8)	0.8(8)	-2.9(9)

Table 4 Bond Lengths for td-17-2.

Atom	Atom	Length/ \AA	Atom	Atom	Length/ \AA
F1	B1	1.387(2)	C11	C12	1.370(3)
F2	B1	1.373(2)	C12	C13	1.423(3)
N1	C14	1.330(3)	C15	C16	1.440(3)

Table 4 Bond Lengths for td-17-2.

Atom	Atom	Length/Å	Atom	Atom	Length/Å
N1	C15	1.318(2)	C16	C17	1.370(3)
N2	C3	1.359(3)	C16	C30	1.515(3)
N2	C14	1.400(2)	C17	C18	1.418(3)
N2	B1	1.564(3)	C18	C19	1.464(2)
N3	C15	1.406(2)	C19	C20	1.379(3)
N3	C18	1.354(2)	C19	C28	1.437(3)
N3	B1	1.563(3)	C20	C21	1.406(3)
C1	C2	1.378(3)	C21	C22	1.366(3)
C1	C14	1.428(3)	C22	C23	1.413(3)
C1	C34	1.520(2)	C23	C24	1.418(3)
C2	C3	1.407(3)	C23	C28	1.430(2)
C3	C4	1.479(3)	C24	C25	1.363(3)
C4	C5	1.376(3)	C25	C26	1.412(3)
C4	C13	1.430(2)	C26	C27	1.372(3)
C5	C6	1.404(3)	C27	C28	1.418(3)
C6	C7	1.366(3)	C29	C30	1.529(3)
C7	C8	1.418(3)	C30	C31	1.536(3)
C8	C9	1.420(3)	C30	C32	1.533(3)
C8	C13	1.423(3)	C33	C34	1.534(3)
C9	C10	1.367(3)	C34	C35	1.532(3)
C10	C11	1.403(3)	C34	C36	1.533(3)

Table 5 Bond Angles for td-17-2.

Atom	Atom	Atom	Angle/°	Atom	Atom	Atom	Angle/°
C15	N1	C14	120.09(16)	C16	C17	C18	109.27(17)
C3	N2	C14	107.31(15)	N3	C18	C17	109.27(15)
C3	N2	B1	129.46(16)	N3	C18	C19	125.11(18)
C14	N2	B1	121.79(16)	C17	C18	C19	125.53(17)
C15	N3	B1	121.97(15)	C20	C19	C18	120.35(17)
C18	N3	C15	107.00(16)	C20	C19	C28	119.90(17)
C18	N3	B1	130.90(15)	C28	C19	C18	119.53(17)
C2	C1	C14	105.56(16)	C19	C20	C21	121.33(18)
C2	C1	C34	128.87(17)	C22	C21	C20	119.87(19)
C14	C1	C34	125.57(17)	C21	C22	C23	121.22(18)
C1	C2	C3	109.16(17)	C22	C23	C24	121.60(17)
N2	C3	C2	108.98(16)	C22	C23	C28	119.53(18)
N2	C3	C4	125.17(16)	C24	C23	C28	118.86(18)

Table 5 Bond Angles for td-17-2.

Atom	Atom	Atom	Angle/°	Atom	Atom	Atom	Angle/°
C2	C3	C4	125.63(17)	C25	C24	C23	121.08(18)
C5	C4	C3	117.12(16)	C24	C25	C26	120.23(19)
C5	C4	C13	119.39(18)	C27	C26	C25	120.28(19)
C13	C4	C3	123.41(17)	C26	C27	C28	120.99(18)
C4	C5	C6	121.87(18)	C23	C28	C19	118.04(17)
C7	C6	C5	119.63(19)	C27	C28	C19	123.47(17)
C6	C7	C8	120.87(19)	C27	C28	C23	118.40(17)
C7	C8	C9	121.14(19)	C16	C30	C29	109.86(15)
C7	C8	C13	119.47(17)	C16	C30	C31	110.17(16)
C9	C8	C13	119.37(18)	C16	C30	C32	109.23(17)
C10	C9	C8	120.73(19)	C29	C30	C31	108.88(18)
C9	C10	C11	119.89(18)	C29	C30	C32	109.10(16)
C12	C11	C10	121.30(19)	C32	C30	C31	109.59(17)
C11	C12	C13	120.30(19)	C1	C34	C33	108.76(15)
C8	C13	C4	118.66(17)	C1	C34	C35	109.95(15)
C8	C13	C12	118.39(17)	C1	C34	C36	110.06(17)
C12	C13	C4	122.89(18)	C35	C34	C33	109.73(17)
N1	C14	N2	123.91(17)	C35	C34	C36	109.70(17)
N1	C14	C1	127.13(17)	C36	C34	C33	108.61(16)
N2	C14	C1	108.96(17)	F1	B1	N2	109.14(15)
N1	C15	N3	123.22(18)	F1	B1	N3	109.75(16)
N1	C15	C16	127.33(17)	F2	B1	F1	111.19(16)
N3	C15	C16	108.98(16)	F2	B1	N2	111.84(16)
C15	C16	C30	126.40(16)	F2	B1	N3	110.19(16)
C17	C16	C15	105.28(16)	N3	B1	N2	104.52(15)
C17	C16	C30	128.32(18)				

Table 6 Torsion Angles for td-17-2.

A	B	C	D	Angle/°	A	B	C	D	Angle/°
N1	C15	C16	C17	-167.84(18)	C15	N1	C14	C1	-177.76(18)
N1	C15	C16	C30	13.1(3)	C15	N3	C18	C17	2.2(2)
N2	C3	C4	C5	115.2(2)	C15	N3	C18	C19	178.91(17)
N2	C3	C4	C13	-68.1(3)	C15	N3	B1	F1	-93.55(19)
N3	C15	C16	C17	4.5(2)	C15	N3	B1	F2	143.69(16)
N3	C15	C16	C30	-174.57(16)	C15	N3	B1	N2	23.4(2)
N3	C18	C19	C20	-50.1(3)	C15	C16	C17	C18	-3.1(2)
N3	C18	C19	C28	135.3(2)	C15	C16	C30	C29	171.96(18)

Table 6 Torsion Angles for td-17-2.

A	B	C	D	Angle/°	A	B	C	D	Angle/°
C1	C2	C3	N2	-0.9(2)	C15	C16	C30	C31	-68.1(2)
C1	C2	C3	C4	173.87(17)	C15	C16	C30	C32	52.3(2)
C2	C1	C14	N1	-178.09(18)	C16	C17	C18	N3	0.7(2)
C2	C1	C14	N2	1.3(2)	C16	C17	C18	C19	-176.06(17)
C2	C1	C34	C33	120.2(2)	C17	C16	C30	C29	-6.9(3)
C2	C1	C34	C35	-119.6(2)	C17	C16	C30	C31	113.1(2)
C2	C1	C34	C36	1.3(3)	C17	C16	C30	C32	-126.5(2)
C2	C3	C4	C5	-58.8(3)	C17	C18	C19	C20	126.1(2)
C2	C3	C4	C13	118.0(2)	C17	C18	C19	C28	-48.5(3)
C3	N2	C14	N1	177.53(16)	C18	N3	C15	N1	168.57(17)
C3	N2	C14	C1	-1.9(2)	C18	N3	C15	C16	-4.13(19)
C3	N2	B1	F1	-68.1(2)	C18	N3	B1	F1	81.8(2)
C3	N2	B1	F2	55.3(3)	C18	N3	B1	F2	-40.9(3)
C3	N2	B1	N3	174.54(16)	C18	N3	B1	N2	-161.25(17)
C3	C4	C5	C6	-179.80(17)	C18	C19	C20	C21	-171.87(17)
C3	C4	C13	C8	-179.23(16)	C18	C19	C28	C23	170.66(16)
C3	C4	C13	C12	-2.3(3)	C18	C19	C28	C27	-12.8(3)
C4	C5	C6	C7	-1.1(3)	C19	C20	C21	C22	0.1(3)
C5	C4	C13	C8	-2.5(3)	C20	C19	C28	C23	-4.0(3)
C5	C4	C13	C12	174.44(18)	C20	C19	C28	C27	172.61(18)
C5	C6	C7	C8	-1.9(3)	C20	C21	C22	C23	-1.6(3)
C6	C7	C8	C9	-175.67(18)	C21	C22	C23	C24	-178.54(18)
C6	C7	C8	C13	2.6(3)	C21	C22	C23	C28	0.3(3)
C7	C8	C9	C10	178.57(18)	C22	C23	C24	C25	175.51(19)
C7	C8	C13	C4	-0.3(3)	C22	C23	C28	C19	2.5(3)
C7	C8	C13	C12	-177.42(17)	C22	C23	C28	C27	-174.24(18)
C8	C9	C10	C11	-1.0(3)	C23	C24	C25	C26	-0.1(3)
C9	C8	C13	C4	177.93(17)	C24	C23	C28	C19	-178.67(17)
C9	C8	C13	C12	0.8(3)	C24	C23	C28	C27	4.6(3)
C9	C10	C11	C12	0.4(3)	C24	C25	C26	C27	2.2(3)
C10	C11	C12	C13	0.8(3)	C25	C26	C27	C28	-0.8(3)
C11	C12	C13	C4	-178.35(18)	C26	C27	C28	C19	-179.15(18)
C11	C12	C13	C8	-1.4(3)	C26	C27	C28	C23	-2.6(3)
C13	C4	C5	C6	3.3(3)	C28	C19	C20	C21	2.7(3)
C13	C8	C9	C10	0.3(3)	C28	C23	C24	C25	-3.3(3)
C14	N1	C15	N3	-0.4(3)	C30	C16	C17	C18	175.90(18)
C14	N1	C15	C16	170.91(17)	C34	C1	C2	C3	-179.48(17)
C14	N2	C3	C2	1.7(2)	C34	C1	C14	N1	1.2(3)

Table 6 Torsion Angles for td-17-2.

A	B	C	D	Angle/°	A	B	C	D	Angle/°
C14N2	C3	C4		-173.11(16)	C34C1	C14N2			-179.43(16)
C14N2	B1	F1		96.4(2)	B1	N2	C3	C2	167.96(16)
C14N2	B1	F2		-140.15(17)	B1	N2	C3	C4	-6.9(3)
C14N2	B1	N3		-21.0(2)	B1	N2	C14N1		10.0(3)
C14C1	C2	C3		-0.2(2)	B1	N2	C14C1		-169.41(15)
C14C1	C34C33			-58.9(2)	B1	N3	C15N1		-15.1(3)
C14C1	C34C35			61.3(2)	B1	N3	C15C16		172.22(15)
C14C1	C34C36			-177.76(18)	B1	N3	C18C17		-173.73(17)
C15N1	C14N2			2.9(3)	B1	N3	C18C19		3.0(3)

Table 7 Hydrogen Atom Coordinates ($\text{\AA} \times 10^4$) and Isotropic Displacement Parameters ($\text{\AA}^2 \times 10^3$) for td-17-2.

Atom	x	y	z	U(eq)
H2	-2169.76	8101.49	7726.22	37
H5	-4734.36	5944.3	7531.22	40
H6	-7010.96	5779.93	6805.23	42
H7	-6429.82	5927.7	5698.62	41
H9	-4369.27	6424.57	4755.46	42
H10	-1568.36	6854.98	4352.83	44
H11	722.63	7010.91	5074.83	43
H12	243.45	6714.22	6194.46	37
H17	5425.83	1310.23	8046.59	36
H20	384.48	827.62	7233.01	37
H21	136.65	-737.45	6497.27	40
H22	2507.05	-1172.27	5874.98	39
H24	5582.57	-720.59	5528.31	40
H25	8112.12	565.53	5537.42	42
H26	8320.17	2312.52	6196.18	42
H27	6046.7	2655.71	6884.52	38
H29A	6018.95	773.55	9266.1	59
H29B	7221.07	1765.91	9613.1	59
H29C	7395.9	1849.98	8837.32	59
H31A	6912.55	4527.04	8604.37	63
H31B	6752.48	4469.83	9378.43	63
H31C	5229.1	5206.05	8890.1	63
H32A	3103.04	3553.14	9596.69	62
H32B	4632.51	2770.08	10069.97	62

Table 7 Hydrogen Atom Coordinates ($\text{\AA}\times 10^4$) and Isotropic Displacement Parameters ($\text{\AA}^2\times 10^3$) for td-17-2.

Atom	x	y	z	U(eq)
H32C	3364.32	1819.62	9726.37	62
H33A	-889.79	6278.6	9485.38	54
H33B	587.92	7143.92	9777.12	54
H33C	1113.22	5812.2	9443.72	54
H35A	3129.41	7343.34	8680.48	56
H35B	2677.95	8751.88	8970.92	56
H35C	2474.07	8819.79	8198.11	56
H36A	-646.4	9703.87	8321.33	61
H36B	-368.34	9510.69	9098.99	61
H36C	-1932.21	8696.43	8828.53	61

Experimental

Single crystals of $\text{C}_{36}\text{H}_{34}\text{BF}_2\text{N}_3$ [**td-17-2**] were []. A suitable crystal was selected and [] on a **XtaLAB AFC12 (RINC): Kappa single** diffractometer. The crystal was kept at 118(20) K during data collection. Using Olex2 [1], the structure was solved with the SHELXT [2] structure solution program using Intrinsic Phasing and refined with the SHELXL [3] refinement package using Least Squares minimisation.

1. Dolomanov, O.V., Bourhis, L.J., Gildea, R.J., Howard, J.A.K. & Puschmann, H. (2009), *J. Appl. Cryst.* 42, 339-341.
2. Sheldrick, G.M. (2015). *Acta Cryst.* A71, 3-8.
3. Sheldrick, G.M. (2015). *Acta Cryst.* C71, 3-8.

Refinement model description

Number of restraints - 0, number of constraints - unknown.

Details:

1. Fixed Uiso

At 1.2 times of:

All C(H) groups

At 1.5 times of:

All C(H,H,H) groups

2.a Aromatic/amide H refined with riding coordinates:

C2(H2), C5(H5), C6(H6), C7(H7), C9(H9), C10(H10), C11(H11), C12(H12),
C17(H17), C20(H20), C21(H21), C22(H22), C24(H24), C25(H25), C26(H26), C27(H27)

2.b Idealised Me refined as rotating group:

C29(H29A,H29B,H29C), C31(H31A,H31B,H31C), C32(H32A,H32B,H32C), C33(H33A,H33B,
H33C), C35(H35A,H35B,H35C), C36(H36A,H36B,H36C)

This report has been created with Olex2, compiled on 2022.04.07 svn.rca3783a0 for OlexSys.

Please let us know if there are any errors or if you would like to have additional features.

7. Cartesian coordinates of the species

revNap-BDP

C	1.13866400	0.45867500	-0.38541500
N	1.25876800	1.83406400	-0.20637900
B	0.00008900	2.75289000	-0.38685900
N	-1.25863100	1.83413500	-0.20625600
C	-1.13862200	0.45874600	-0.38535900
N	-0.00000100	-0.18398700	-0.46583900
C	2.43617000	-0.13286400	-0.37071100
C	3.31364600	0.91638100	-0.17113500
C	2.57737800	2.11763500	-0.08242600
C	-2.57722100	2.11777800	-0.08223300
C	-3.31357500	0.91658700	-0.17107500
C	-2.43616600	-0.13270900	-0.37067800
C	2.71851300	-1.54903800	-0.56554300
C	-2.71860300	-1.54885400	-0.56558700
C	2.05676300	-2.22818400	-1.56779300
C	2.33017200	-3.57465300	-1.84571500
C	3.27386500	-4.24886600	-1.12125500
C	3.96300300	-3.60848800	-0.06871100
C	3.67984000	-2.24469200	0.23249300
C	-3.67999000	-2.24448300	0.23240000
C	-3.96324300	-3.60824400	-0.06888100
C	-3.27413500	-4.24861400	-1.12144900
C	-2.33038500	-3.57442800	-1.84585900
C	-2.05688600	-2.22799300	-1.56786300
C	-4.33324000	-1.65928300	1.34110100
C	-5.24808000	-2.36347100	2.07761400
C	-5.55792000	-3.69581500	1.74995200
C	-4.92057300	-4.30358400	0.70407900
C	4.92027400	-4.30385400	0.70429800
C	5.55764800	-3.69607400	1.75014800
C	5.24789600	-2.36369200	2.07773700
C	4.33311500	-1.65947900	1.34117400
C	3.19388200	3.47420000	0.16601300
C	4.71563500	3.37435100	0.02324900
C	2.70158100	4.53104600	-0.82815700
C	2.88313800	3.90732500	1.60771400
C	-3.19364500	3.47436800	0.16627100
C	-2.70065900	4.53138200	-0.82738100
C	-4.71534000	3.37478300	0.02271000
C	-2.88360100	3.90707900	1.60825000

F	0.00003900	3.26503300	-1.67632700
F	0.00018400	3.76545000	0.55917500
H	4.38690300	0.84603000	-0.13170300
H	-4.38683700	0.84630900	-0.13166800
H	1.32861500	-1.69617700	-2.16563500
H	1.79816200	-4.07138000	-2.64909800
H	3.50281200	-5.28678600	-1.33936300
H	-3.50314900	-5.28650700	-1.33961400
H	-1.79839700	-4.07115000	-2.64926100
H	-1.32869300	-1.69600400	-2.16566700
H	-4.08618500	-0.64370800	1.62092700
H	-5.73067900	-1.89361200	2.92732000
H	-6.28799100	-4.24106000	2.33723000
H	-5.13259000	-5.33844000	0.45577100
H	5.13222200	-5.33873800	0.45604700
H	6.28767300	-4.24133900	2.33746500
H	5.73051500	-1.89382100	2.92742500
H	4.08612700	-0.64387200	1.62094300
H	5.14978900	4.36198600	0.19111000
H	5.15266400	2.69505600	0.75853300
H	5.00801100	3.04418000	-0.97639100
H	3.26597400	5.45301600	-0.66542400
H	1.64594200	4.75601700	-0.70852600
H	2.86752700	4.20681000	-1.85774200
H	3.26994500	3.17555200	2.32176000
H	3.37165600	4.86549900	1.80576100
H	1.81349400	4.02316200	1.76727100
H	-3.26493400	5.45342800	-0.66466700
H	-1.64502600	4.75609100	-0.70718800
H	-2.86618200	4.20745700	-1.85713200
H	-5.14943600	4.36242800	0.19066200
H	-5.15283400	2.69531900	0.75756200
H	-5.00726300	3.04496900	-0.97718000
H	-3.27087800	3.17516500	2.32189700
H	-1.81403500	4.02275000	1.76841200
H	-3.37211600	4.86525600	1.80629000

Nap-BDP

C	-1.14207000	1.73926100	-0.33242300
N	-1.23997200	0.36031900	-0.49985400
B	-0.00000500	-0.53354400	-0.82523500
N	1.23998600	0.36030100	-0.49986700

C	1.14210400	1.73925100	-0.33246200
N	0.00002300	2.38571800	-0.26267700
C	-2.45488300	2.27818500	-0.14234200
C	-3.30412200	1.19599900	-0.17272100
C	-2.53701800	0.02468100	-0.39951800
C	2.53702800	0.02465200	-0.39957100
C	3.30415700	1.19596500	-0.17282000
C	2.45493300	2.27816100	-0.14242700
F	-0.00000500	-0.81403500	-2.19649300
F	-0.00001000	-1.67882400	-0.07030200
C	4.28703600	-3.80740600	-1.03651100
C	4.63926900	-3.08734500	0.12572200
C	4.02363000	-1.82972600	0.38461000
C	3.07934900	-1.32145300	-0.56053300
C	2.74809200	-2.07232600	-1.66764500
C	3.35169000	-3.31597400	-1.90437100
C	5.58059000	-3.59941100	1.04680400
C	5.88825700	-2.91775100	2.19176700
C	5.24931800	-1.69638100	2.47109600
C	4.33848800	-1.16969300	1.59437100
C	-4.28713500	-3.80731100	-1.03655400
C	-3.35177800	-3.31588200	-1.90440400
C	-2.74814100	-2.07225900	-1.66764500
C	-3.07936700	-1.32140800	-0.56050800
C	-4.02365600	-1.82968300	0.38462700
C	-4.63933800	-3.08727400	0.12570400
C	-4.33848300	-1.16967900	1.59441200
C	-5.24932600	-1.69636500	2.47112600
C	-5.88830900	-2.91770300	2.19176000
C	-5.58067200	-3.59933700	1.04677400
C	-2.80718600	3.72499300	0.07087000
C	-2.26727500	4.56812900	-1.09024300
C	-4.32259300	3.89443000	0.14733900
C	-2.18534100	4.20907800	1.38707600
C	2.80725600	3.72495500	0.07085600
C	4.32267800	3.89441900	0.14695000
C	2.26700600	4.56826100	-1.08997000
C	2.18574600	4.20881100	1.38731000
H	-4.37806900	1.20190400	-0.08009100
H	4.37810800	1.20185400	-0.08023300
H	4.76587800	-4.76319100	-1.22262300
H	2.02589500	-1.68559300	-2.37427000
H	3.07759000	-3.87687500	-2.79031500
H	6.04807700	-4.55466900	0.83139800

H	6.60917500	-3.32305600	2.89261600
H	5.47043800	-1.17386300	3.39502600
H	3.83423600	-0.24268200	1.83684700
H	-4.76600900	-4.76307500	-1.22269300
H	-3.07770100	-3.87676300	-2.79036800
H	-2.02594100	-1.68552600	-2.37426700
H	-3.83419700	-0.24269400	1.83691500
H	-5.47042200	-1.17387000	3.39507400
H	-6.60923800	-3.32300600	2.89259900
H	-6.04819300	-4.55457200	0.83134100
H	-2.53842100	5.61738600	-0.94387600
H	-1.18158000	4.49506400	-1.15194300
H	-2.68948000	4.23585000	-2.04180700
H	-4.56788100	4.94888900	0.29456600
H	-4.74703100	3.33294700	0.98360200
H	-4.80883400	3.56165800	-0.77319200
H	-2.55323500	3.62032500	2.23110200
H	-1.09944800	4.12441900	1.35587400
H	-2.44859000	5.25649100	1.55950000
H	4.56798100	4.94886900	0.29421200
H	4.74735000	3.33287100	0.98305000
H	4.80868800	3.56174000	-0.77373700
H	2.53821900	5.61749100	-0.94353400
H	1.18129200	4.49522200	-1.15134200
H	2.68891100	4.23611300	-2.04171300
H	1.09984800	4.12407900	1.35640000
H	2.55391900	3.61996300	2.23114700
H	2.44896400	5.25621900	1.55980900

8. Reference

- [1] M.J.T. Frisch, G. W.; Schlegel, H. B.; Scuseria, G. E.; Robb, M. A.; Cheeseman, J. R.; Scalmani, G.; Barone, V.; Mennucci, B.; Petersson, G. A.; Nakatsuji, H.; Caricato, M.; Li, X.; Hratchian, H. P.; Izmaylov, A. F.; Bloino, J.; Zheng, G.; Sonnenberg, J. L.; Hada, M.; Ehara, M.; Toyota, K.; Fukuda, R.; Hasegawa, J.; Ishida, M.; Nakajima, T.; Honda, Y.; Kitao, O.; Nakai, H.; Vreven, T.; Montgomery, J. A., Jr.; Peralta, J. E.; Ogliaro, F.; Bearpark, M.; Heyd, J. J.; Brothers, E.; Kudin, K. N.; Staroverov, V. N.; Keith, T.; Kobayashi, R.; Normand, J.; Raghavachari, K.; Rendell, A.; Burant, J. C.; Iyengar, S. S.; Tomasi, J.; Cossi, M.; Rega, N.; Millam, J. M.; Klene, M.; Knox, J. E.; Cross, J. B.; Bakken, V.; Adamo, C.; Jaramillo, J.; Gomperts, R.; Stratmann, R. E.; Yazyev, O.; Austin, A. J.; Cammi, R.; Pomelli, C.; Ochterski, J. W.; Martin, R. L.; Morokuma, K.; Zakrzewski, V. G.; Voth, G. A.; Salvador, P.; Dannenberg, J. J.; Dapprich, S.; Daniels, A. D.; Farkas, O.; Foresman, J. B.; Ortiz, J. V.; Cioslowski, J.; Fox, D. J., Gaussian 09, revision D01, (2013).
- [2] C. Adamo, V. Barone, Toward reliable density functional methods without adjustable parameters: The PBE0 model, *J Chem Phys*, 110(1999) 6158-70.
- [3] V. Barone, M. Cossi, J. Tomasi, A new definition of cavities for the computation of solvation free energies by the polarizable continuum model, *J Chem Phys*, 107(1997) 3210-21.
- [4] J. Tomasi, B. Mennucci, R. Cammi, Quantum mechanical continuum solvation models, *Chem Rev*, 105(2005) 2999-3093.
- [5] T. Lu, F. Chen, Multiwfn: a multifunctional wavefunction analyzer, *J Comput Chem*, 33(2012) 580-92.
- [6] E.R. Johnson, S. Keinan, P. Mori-Sánchez, J. Contreras-García, A.J. Cohen, W. Yang, Revealing Noncovalent Interactions, *J Am Chem Soc*, 132(2010) 6498-506.
- [7] W. Humphrey, A. Dalke, K. Schulten, VMD: Visual molecular dynamics, *J Mol Graph*, 14(1996) 33-8.